CONF-841201--23

STRESS CORROSION CRACK GROWTH RATES IN TYPE 304 STAINLESS STEEL IN SIMULATED BWR ENVIRONMENTS*

J. Y. Park, W. E. Ruther, T. F. Kassner, and W. J. Shack

Materials Science and Technology Division
Argonne National Laboratory
Argonne, Illinois 60439

CONF-841201--23

November 1984

TI85 004026

DISCLAIMER

To be presented at the Symposium on the Crack Growth Behavior and Performance of Structural Components Susceptible to Stress Corrosion Cracking, ASME Winter Annual Meeting, New Orleans, LA, December 9-13, 1984, and submitted for publication in ASME Journal of Engineering Materials and Technology.

*Work supported by the U. S. Nuclear Regulatory Commission.

STRESS CORROSION CRACK GROWTH RATES IN TYPE 304 STAINLESS STEEL IN SIMULATED BWR ENVIRONMENTS*

J. Y. Park, W. E. Ruther, T. F. Kassner, and W. J. Shack

Materials Science and Technology Division
Argonne National Laboratory
Argonne, Illinois 60439

ABSTRACT

Stress corrosion cracking of Type 304 stainless steel has been studied with fracture-mechanics-type standard 25.4-mm-thick compact tension specimens in simulated boiling-water reactor environments at 289°C and 8.3 MPa. Tests were performed with either constant or cyclic loading. The latter tests used a positive sawtooth waveform with an unloading time of 1 or 5 s, a load ratio R (minimum load to maximum load) of 0.2 to 0.95, and a frequency f of 8×10^{-4} to 1×10^{-1} Hz. Crack lengths and crack growth rates were determined by the compliance method; crack mouth opening displacement was measured with in-situ clip gauges. Fractography was used to examine the mode of cracking and to confirm the compliance method for crack length determination. The test environments were high-purity deionized water with 0.2- to 8-ppm dissolved oxygen, and water with 0.2-ppm dissolved oxygen and 0.1-ppm sulfate (as H_2SO_4). Two heats with a carbon content of 0.06 wt % were investigated in solution-heat-treated and furnace-sensitized conditions. Degree of sensitization varied from ~0 to 20 C/cm^2 as measured by the electrochemical potentiokinetic polarization method.

The first heat was tested in water with 0.2- and 8-ppm dissolved oxygen and with 0.2-ppm dissolved oxygen and 0.1-ppm sulfate. The loading conditions

*Work supported by the U. S. Nuclear Regulatory Commission.

encompassed the range f = 8 x 10^{-2} to 8 x 10^{-4} Hz, K_{max} = 28 to 72 MPa•$m^{1/2}$, and R = 0.95. Under these conditions, the crack growth rates were ~0 to 3 x 10^{-9} m/s. The effects of water chemistry transients which produced changes in the concentration of dissolved oxygen or sulfate in the environment were also investigated.

The second heat was tested in water with 8-ppm dissolved oxygen. The influence of load ratio and frequency was investigated over the range R = 0.5 to 1.0 and f = 1 x 10^{-1} to 2 x 10^{-3} Hz, at maximum stress intensity K_{max} = 28 to 38 MPa•$m^{1/2}$. Under these conditions, crack growth rates varied from 1 x 10^{-10} to 3 x 10^{-9} m/s. Crack growth rate increased significantly at low R values. However, the growth rate at R = 0.95 was not significantly different from that under constant load. Correlation of the crack growth rate data with crack-tip strain rates is discussed.

INTRODUCTION

A significant amount of fracture-mechanics-type crack growth rate data for stress corrosion cracking (SCC) of sensitized stainless steels is now available [1]. Much of this data has been obtained under constant loading conditions on rather highly sensitized materials in high-purity environments. Recent data from slow-strain-rate tests [2,3] suggest that low levels of impurity anions (sulfate, chloride, carbonate, etc.), which can be introduced by decomposition of ion exchange resins or condenser in-leakage, can have a significant effect on susceptibility even though the water chemistry remains within the limits in Nuclear Regulatory Commission Regulatory Guide 1.56. In addition, even under "steady" load, the stresses in piping may not be truly constant because of pressure and temperature fluctuations and mechanical vibrations. Although in most cases the stresses are small and are

generally negligible from a fatigue standpoint, small variations in stress can have a significant effect on stress corrosion crack growth [4]. A program to study the effects of impurities [both at dissolved-oxygen levels corresponding to conventional boiling water reactor (BWR) water chemistry and at the lower dissolved-oxygen levels corresponding to a BWR operating with hydrogen additions to the feedwater] and the effect of small cyclic loads superposed on a high mean load ("high R" cyclic loading) is currently in progress at Argonne National Laboratory. Recent results from this work are reported in this paper.

TEST METHODS

Tests have been performed on two heats of Type 304 stainless steel. The compositions are given in Table I. The alloys initially were solution annealed at 1050°C for 0.5 h (water quenched). For heat No. 30956, subsequent heat treatments of 12 h at 700°C resulted in moderate sensitization, EPR = 20 C/cm^2, while 0.25 h at 700°C plus 24 h at 500°C resulted in light sensitization, EPR = 2 C/cm^2. For heat 10285, a heat treatment of 0.17 h at 700°C followed by 24 h at 500°C gave an EPR value of 1.4 C/cm^2, and 17 h at 700°C followed by 250 h at 450°C produced an EPR value of 1.8 C/cm^2.

The tests were performed in autoclave systems installed in MTS servo-hydraulic load frames. The autoclave systems have a volume of 6 ℓ. The flow rate through the autoclave is 0.5-1.0 ℓ/h. The dissolved-oxygen concentrations were established by bubbling an appropriate oxygen/nitrogen gas mixture through deoxygenated/deionized feedwater (conductance of $\lesssim$0.2 μS/cm) contained in a 120-ℓ stainless steel tank. In tests with impurities, sulfuric acid was added to the feedwater prior to sparging with the gas mixture to ensure adequate mixing. The oxygen concentration and the pressure of the cover gas

in the feedwater tank were adjusted to provide the desired autoclave effluent dissolved-oxygen content. Leeds and Northrup Model 7931 meters were used to determine the dissolved-oxygen concentration of the water, and the results were verified by colorimetric (Chemetrics ampules) and conductometric (thallium column) techniques. Three specimens were loaded in series, and the crack lengths were determined during the test by means of compliance measurements obtained from high-temperature clip gauges mounted on each specimen. The crack lengths obtained from the compliance measurements were compared with those measured on the fracture surfaces during post-test examination.

The specimens from heat No. 30956 were tested in the solution-annealed and sensitized conditions. Sensitization levels were measured using the electrochemical-potentiodynamic reactivation (EPR) technique. The EPR values for the solution-annealed and the sensitized specimens from this heat were 0, 2, and 20 C/cm^2. The EPR values for the specimens from the second heat (No. 10285) were 1.4 and 1.8 C/cm^2. The tests on heat No. 30956 were intended primarily to investigate the effect of impurities and dissolved-oxygen content on the crack growth rates. The tests on heat No. 10285 were intended to determine the effect of the loading history on the crack growth rates.

RESULTS

Baseline tests on heat No. 30956 were performed in high-purity water with 8-ppm dissolved oxygen at 289°C. Three 1TCT specimens were stressed at a load ratio of 0.95 and an initial K_{max} of 28 $MPa \cdot m^{1/2}$ under a positive sawtooth waveform. No fatigue precracking was introduced into these specimens. The cyclic frequencies, which result from periods of slowly rising load followed by a rapid (~1-s) decrease in load, were 8×10^{-2}, 8×10^{-3}, and 8×10^{-4} Hz for different phases of the experiment. The crack growth rate data are

summarized in Table II, and the dependence of the crack growth rate on K_{max} is shown in Fig. 1.

As expected, the most heavily sensitized material showed the highest crack growth rate. The crack growth rate increased by about an order of magnitude as the cyclic frequency was increased from $\sim 10^{-2}$ to $\sim 10^{-1}$ Hz. For this heat of material in oxygenated high-purity water and these loading conditions, the crack growth rates appear to be sensitive to small, superposed cyclic loading, although the measured crack growth rates are within the scatter band obtained for a number of heats of material under constant loading conditions [1].

The effect of dissolved-oxygen concentration on the crack growth properties of the same heat (No. 30956) was evaluated in a similar experiment at 289°C, in which three 1TCT specimens (EPR = 0, 2, and 20 C/cm^2) were loaded at an R value of 0.95 and a frequency of 8×10^{-2} Hz under a positive sawtooth waveform. The specimens were fatigue-precracked in air at 289°C. The dissolved-oxygen level was fixed at ~0.2 ppm for ~1000 h, decreased to 0.02 ppm for ~600 h, and then increased back to 0.2 ppm. The crack length as a function of time is shown in Fig. 2. The curves clearly indicate that crack growth in the three specimens virtually ceased over the ~600-h time interval at the low dissolved-oxygen concentration. Crack growth in the three specimens resumed at approximately the initial rates after the dissolved-oxygen concentration was increased to the 0.2-ppm value. The crack lengths, stress intensity values, and crack growth rates for the time periods at the different dissolved-oxygen concentrations in the water during the transient are given in Table III.

The crack growth rate for the material with EPR = 20 C/cm^2 in water with 0.2-ppm dissolved oxygen is approximately half of that obtained in water with

8-ppm dissolved oxygen, as expected. However, the crack growth rate of the material with EPR = 2 C/cm^2 is approximately an order of magnitude higher at the lower dissolved-oxygen concentrations. Measurable crack growth rates were also observed in the solution-annealed specimen at the lower dissolved-oxygen level, whereas no measurable crack growth was detected for the baseline tests in 8-ppm dissolved oxygen water described above. We believe this somewhat unexpected behavior results from the 2 to 3 mm-deep fatigue precracks in the specimens used to facilitate SCC initiation in the 0.2-ppm dissolved-oxygen environment. It appears that once a sharp crack (or tight crevice) is introduced by fatigue precracking, propagation can occur under conditions that would not normally be considered to lead to environmentally assisted cracking. It should be noted, however, that even in CERT tests the material with EPR = 2 C/cm^2 shows more susceptibility in water with 0.2-ppm dissolved oxygen than with 8-ppm dissolved oxygen [2].

Fractographic examination of the specimens after the completion of the test showed that the crack mode was primarily intergranular in the sensitized specimens and transgranular in the solution-annealed specimen. However, the observed decrease in crack growth rate in the solution-annealed specimen when the oxygen was decreased (Fig. 2) indicates that even the transgranular growth, once initiated, is strongly influenced by the environment. The unmeasurably low crack growth rates during the low-oxygen phase of this experiment (Fig. 2) also suggest that the compliance measurements did not influence the rate of crack growth.

Another crack growth experiment was performed to investigate the effect of impurities, e.g., H_2SO_4 from decomposition of ion exchange resins, on the crack growth rate of the material. Three 1TCT specimens with EPR values of 0, .2, and 20 C/cm^2 were fatigue-precracked and tested in water containing

0.2-ppm dissolved oxygen and 0.1-ppm sulfate (as H_2SO_4), which results in an environment within the Nuclear Regulatory Guide 1.56 limits on pH and specific conductance for BWR operation at >1% power. The specimens were again loaded by a positive sawtooth waveform with an initial K_{max} of 28 MPa•$m^{1/2}$, an R value of 0.95, and a frequency of 8×10^{-2} Hz. The crack length as a function of time for the initial portion of the experiment is shown in Fig. 3. The lightly sensitized specimen (EPR = 2 C/cm^2) exhibits the highest crack growth rate in the impurity environment. Crack growth initiated in the solution-annealed specimen at a K_{max} value of ~34 MPa•$m^{1/2}$; and for a given K_{max} greater than this initiation value, the growth rate in the solution-annealed specimen is somewhat larger than for the lightly sensitized specimen. The crack growth rate for the more highly sensitized specimen (EPR = 20 C/cm^2) is significantly lower than those for the other two specimens, as shown in Fig. 4.

After ~6000 h of testing, the sulfate level in the feedwater was reduced to a very low level, and measurements of the crack length in the three specimens were made over a period of ~200 h. After this time interval, the sulfate level was again increased to 0.1 ppm, and crack growth in the specimens was determined over a period of ~370 h.

The crack lengths as a function of time for this portion of the test are also shown in Fig. 4. The stress intensity values for the lightly sensitized specimen (EPR = 2 C/cm^2) at different times in the experiment are noted on the figure. These values, along with similar information for the other specimens, are also given in Table IV. It is clear from Fig. 4 and Table IV that removal of sulfate had virtually no effect on crack growth in the solution-annealed (EPR = 0) and the more heavily sensitized (EPR = 20 C/cm^2) specimens. The crack growth rate of the lightly sensitized specimen decreased by a factor of

~4 over an ~600-h period after sulfate was removed from the feedwater; however, the rate in high-purity water increased over the next 600 h to the initial value observed in the water with 0.1-ppm sulfate. A further increase in the crack growth rate occurred at ~7300 h when sulfate was again added to the feedwater. Since the actual crack length in the EPR = 2 C/cm^2 specimen grew from ~9 to 13 mm during the transient water chemistry experiment, the stress intensity factor increased from ~49 to ~63 $MPa \cdot m^{1/2}$, which has some effect on the growth rate over the duration of the test. Crack growth rates versus K_{max} are shown in Fig. 5. The data shown suggest that the crack growth rate varies as $(K_{max})^{4.0}$ under constant water chemistry (0.2-ppm oxygen and 0.1-ppm sulfate). Thus, the increase in the stress intensity factor from 53 to 59 $MPa \cdot m^{1/2}$ during the time period when no sulfate was present in the water would account for a factor of 1.5 increase in the crack growth rate. The crack growth rate during the last half of this period was a factor of three higher than that during the first half. If we assume that the initial decrease in the crack growth rate was due to the change in crack tip chemistry associated with the removal of sulfate from the bulk water, it is possible that sulfate or perhaps other sulfur species slowly desorbed from the oxide on the walls of the crack, migrated to the crack tip zone, and subsequently influenced the crack growth process.

Qualitatively the effect of the dissolved oxygen and the effect of the sulfate additions observed in the fracture-mechanics crack growth rate tests are for the most part consistent with the crack growth information obtained from constant extension rate tension (CERT) tests on the same heat of material [2]. However, a much larger relative reduction in crack growth rates is observed in the fracture-mechanics crack growth rate tests when the dissolved oxygen is reduced to very low levels than in the corresponding CERT tests [2].

It is believed that the effective crack tip strain rates in CERT specimens are larger than those for fracture-mechanics-type specimens, and faster crack propagation rates are observed for CERT tests. The large relative reduction in crack growth rates in the fracture-mechanics crack growth tests due to reduced dissolved oxygen concentration suggests that there may exist a threshold crack tip strain rate for stress corrosion cracking.

The tests on heat No. 10285 were performed in high-purity water with 8 ppm dissolved at 289°C. The specimens were furnace-heat-treated to give EPR values of 1.4 and 1.8 C/cm^2. Crack growth rate tests were performed for K_{max} values between 29 and 40 $MPa \cdot m^{1/2}$, R values from 0.5 to 1, and frequencies f of 0, 1×10^{-3}, 2×10^{-3}, and 1×10^{-1} Hz. The crack growth rates for the different loading conditions are summarized in Table V. Post-test examination of the fracture surfaces showed that for this environment and level of sensitization only the tests under constant load (R = 1) provided true intergranular cracking; at other load ratios the cracks were primarily transgranular. Although the crack growth mode changed as R decreased from 1 to 0.95, the magnitude of the crack growth rate was relatively unchanged by the superposed cyclic loading even at frequencies as high as 0.1 Hz. This contrasts sharply with the behavior observed for the more heavily sensitized specimen from heat No. 30956 in the same environment (cf. Fig. 1), which showed an order of magnitude change in growth rate for loading at ~0.1 Hz.

Empirical correlations for SCC crack growth under constant load are usually expressed as a function of the stress intensity factor, whereas fatigue crack growth is expressed as a function of $\Delta K = K_{max} - K_{min}$ and R, or equivalently, in terms of an effective stress intensity K_{eff} that depends on K_{max} and R. Recently Gilman has considered crack growth in sensitized stainless steels [5] by means of linear superposition of the constant-load

crack growth rates with the fatigue crack growth rate to predict crack growth under more complex loading histories. In considering data obtained on multiple heats of materials, he obtained an estimate of the form

$$\dot{a} = A_1 \int_o^T [K(t)]^3 \, dt + A_2 \, K_{eff}^4 / T \, , \tag{1}$$

where

$$K_{eff} = \frac{\Delta K}{1 - \frac{R}{2}} \, , \tag{2}$$

$\dot{a}$ is crack growth rate, A_1 and A_2 are constants, and T is the period of the cycling loading.

Ford [4] has proposed that the stress corrosion crack growth rate in the environments of interest here is proportional to a power ($n \simeq 0.5$) of the crack tip strain rate, i.e.,

$$\dot{a} = A \, \dot{\varepsilon}_T^{\,n} \, , \tag{3}$$

where $\dot{\varepsilon}_T$ is the crack tip strain rate. This relation is consistent with data obtained from CERT tests at different strain rates [6]. Application of this approach to fracture-mechanics crack growth tests requires an expression for the crack tip strain rate.

For cyclic applied loads of sufficiently high frequency (and sufficiently low R values), the strains are imposed by the external loading mechanism. An estimate of crack tip strain rates in this case has been obtained by Scott and Truswell [7], which is of the form

$$\dot{\varepsilon}_T = - 1/\tau \ln [1 - (1- R)^2/2], \quad (4)$$

where τ is the rise time for the tensile portion of the load cycle. Equation (4), since it neglects constant-load creep, predicts $\dot{\varepsilon}_T = 0$ for the constant-load case. It also predicts that the crack-tip strain rate is independent of the value K and hence, together with Eq. (3), predicts that the crack growth rate is independent of K.

Under constant applied loads, the crack-tip strain rate is determined by time-dependent plastic deformation, i.e., creep near the crack tip. Rewriting the usual empirical representation for the crack growth under constant load

$$\dot{a} = BK^m \quad (5)$$

as

$$\dot{a} = A \left(\frac{B}{A} K^m\right) \quad (6)$$

suggests that the creep contribution to the crack-tip strain rate is

$$\dot{\varepsilon}_T = CK^{m/n}, \quad (7)$$

where A, B, m, and n are constants and $C = [B/A]^{1/n}$. Since A can be determined independently by either rapid straining tests [4] or CERT tests [6], the constant C can be determined from constant-load crack growth rate tests. The crack tip strain rate under cyclic loading can then be approximated as the sum of Eqs. (4) and (7). The total crack growth rate can then be obtained by superposition of Eq. (3) and the fatigue crack growth rate

$$\dot{a} = A \left\{CK^{m/n} - 1/\tau \ln [1-(1-R)^2/2]\right\}^n + D K_{eff}^4/T. \quad (8)$$

Although in theory A, C, and D can be determined from CERT tests, constant-load stress corrosion crack growth rate tests, and fatigue crack growth rate tests, in practice such a complete set of data is seldom available on a single heat of material. The data in Table V were analyzed by obtaining estimates of the form of Eqs. (1) and (8) and determining the coefficients A_1 and A_2 or A and D by a least squares fit to the data. Comparisons of the crack growth rates predicted by Eqs. (1) and (8) are shown in Figs. 6 and 7. For both representations the agreement in most cases is within a factor of two. Both models also predict that except for the constant load cases and for loading with R = 0.95 and f = 2×10^{-3} Hz, the crack growth is dominated by the transgranular (fatigue) term. However, the scatter in the data is too large to determine whether either representation gives a significantly better fit.

CONCLUSIONS

Fracture-mechanics-type crack growth rate experiments have confirmed CERT test results with regard to the deleterious effect of sulfate in the environment on SCC susceptibility. A transient chemistry test in which the sulfate was present for a time and then removed indicated that intrusions may have significant long-term effects that can persist even after the sulfate level in the bulk water is reduced. Significant crack growth in precracked specimens has been obtained even in solution-annealed materials in high-purity environments at moderate stress intensity factors ($K \geq 32$ MPa$\cdot m^{1/2}$). This is consistent with the results reported in Ref. 8 (which were obtained at much higher nominal K values and in environments with 8-ppm dissolved oxygen) and strongly suggests that once a crack has initiated either by fatigue or by stress corrosion, it will continue to propagate under loading and environmental conditions in which smooth, uncracked specimens appear resistant to

environmentally assisted cracking. However, the results of a test in which the oxygen level was reduced to 20 ppb suggest that lowering the oxygen level can arrest the growth of existing cracks at least under some circumstances.

The effect of loading history on the crack growth rate appears to be complex. In some tests a very significant effect of small, superposed cyclic loading on the crack growth rate was observed, whereas in other tests virtually no effect was observed. However, the circumstances that can lead to a significant interaction are not understood. Superposition of stress corrosion crack rate data obtained under constant load with fatigue crack growth data using both the conventional approach of Gilman [5] and the crack tip strain rate approach of Ford [4] appears to give fairly reasonable predictions of the crack growth rate under more complex loading histories, but more data are required before any real assessment can be made.

ACKNOWLEDGMENTS

The authors wish to acknowledge the assistance of W. F. Burke, R. R. Schlueter, D. J. Dorman, J. J. Puro, and W. K. Soppet in various aspects of the experimental work. This research was supported by the Materials Engineering Branch of the U. S. Nuclear Regulatory Commission, Office of Nuclear Regulatory Research.

REFERENCES

1. R. Horn et al., The Growth and Stability of Stress Corrosion Cracks in Large-Diameter BWR Piping, EPRI NP-2472, Vol. 2, Electric Power Research Institute (July 1982).
2. W. E. Ruther, W. K. Soppet, and T. F. Kassner, in Environmentally Assisted Cracking in Light Water Reactors: Annual Report, October 1982-September 1983, NUREG/CR-3806, ANL-84-36, Argonne National Laboratory (June 1984).

3. M. E. Indig and R. B. Davis, The Effect of Aqueous Impurities on the Stress Corrosion Cracking of Austenitic Stainless Steel in High Temperature Water, Paper No. 128, Corrosion 83, National Assoc. Corrosion Engineers, Houston, TX (1983).

4. F. P. Ford, Mechanisms of Environmental Cracking in Systems Peculiar to the Power Generation Industry, EPRI NP-2589, Electric Power Research Institute (1982).

5. J. Gilman, Interpretation of Corrosion Fatigue in LWR Environments, EPRI RP-2006 Project Review, Electric Power Research Institute (Oct. 1983).

6. P. S. Maiya and W. J. Shack, in Environmentally Assisted Cracking in Light Water Reactions: Annual Report, October 1982-September 1983, NUREG/CR-3806, ANL-84-36, Argonne National Laboratory (June 1984).

7. P. M. Scott and A. E. Truswell, "Corrosion Fatigue Crack Growth in Reactor Pressure Vessel Steels in PWR Primary Water," J. Pressure Vessel Technology 105, 245-255 (August 1983).

8. J. Alexander et al., Alternative Alloys for BWR Pipe Applications, EPRI NP-2671-LD, Electric Power Research Institute (October 1982).

TABLE I. Chemical Composition of Type 304 Stainless Steel[a]

Heat No.	C	Cr	Ni	Mn	Si	Mo	Cu	N	P	S
30956	0.06	18.99	8.00	1.54	0.48	0.44	0.19	0.10	0.019	0.007
10285	0.06	18.37	8.48	1.58	0.59	0.38	0.27	0.08	0.028	0.011

[a]Values given in weight percent.

TABLE II. Crack Growth Rate Results on Heat No. 30956 in High-Purity Water with 8-ppm Oxygen at 289°C and an R Value of 0.95

EPR, C/cm^2	Loading Time, s	Frequency,[a] Hz	K_{max}, $MPa \cdot m^{1/2}$	Crack Growth Rate, $m \cdot s^{-1}$
20	12	8×10^{-2}	28	7.5×10^{-10}
20[b]	12	8×10^{-2}	33.8	1.0×10^{-9}
20[b]	12	8×10^{-2}	35.2	1.2×10^{-9}
20	126	8×10^{-3}	34	1.2×10^{-10}
20	126	8×10^{-3}	38	1.5×10^{-10}
20	126	8×10^{-3}	50	4.7×10^{-10}
20	126	8×10^{-3}	61	1.1×10^{-9}
20	126	8×10^{-3}	64	1.7×10^{-9}
20	1260	8×10^{-4}	28	1.2×10^{-10}
20	1260	8×10^{-4}	67	1.9×10^{-9}
20	1260	8×10^{-4}	70	3.2×10^{-9}
20	1260	8×10^{-4}	72	3.3×10^{-9}
2	12	8×10^{-2}	28	4.7×10^{-11}
2	1260	8×10^{-4}	26	$<1.6 \times 10^{-11}$
0	12	8×10^{-2}	28	0
0	126	8×10^{-3}	24-45	0
0	1260	8×10^{-4}	24-25	0

[a]Frequency is based primarily on the loading time, since the load decrease occurs within ~1 s.
[b]Duplicate specimens from another crack growth experiment.

TABLE III. Crack Growth Results for Type 304 SS (Heat No. 30956) Specimens[a] during an Experiment[b] in Which the Dissolved-Oxygen Concentration of the Feedwater Was Decreased from 0.2 to 0.02 ppm and Then Returned to the Initial Value

	Water Chemistry		Specimen #22 (EPR = 0 C/cm^2)			Specimen #20 (EPR = 2 C/cm^2)			Specimen #21 (EPR = 20 C/cm^2)		
Time, h	Oxygen,[c] ppm	Cond., µS/cm	Crack Length, mm	K_{max}, MPa•m$^{1/2}$	Growth Rate, m•s^{-1}	Crack Length, mm	K_{max}, MPa•m$^{1/2}$	Growth Rate, m•s^{-1}	Crack Length, mm	K_{max}, MPa•m$^{1/2}$	Growth Rate, m•s^{-1}
218	0.16	0.10	0.81	26.9	–	1.63	28.0	–	2.08	28.7	–
960	0.23	0.11	1.07	27.3	9.8×10^{-11}	2.54	29.3	3.4×10^{-10}	2.87	29.9	3.1×10^{-11}
1037	<0.02	0.10	1.07	27.3	–	2.46	29.3	–	2.84	29.9	–
1637	<0.02	0.09	1.09	27.3	~0	2.46	29.3	~0	2.79	29.8	~0
1807	0.24	0.10	1.24	27.5	–	2.92	30.0	–	3.28	30.5	–
2304	0.32	0.16	1.57	28.0	1.8×10^{-10}	3.10	30.3	4.5×10^{-11}	3.78	31.3	2.8×10^{-10}
2382	0.21	0.13	1.60	28.0	–	3.15	30.3	–	3.76	31.3	–
2856	0.25	0.14	1.88	28.4	1.6×10^{-10}	3.86	31.5	[d] 4.2×10^{-10}	4.11	31.9	[d] 2.0×10^{-10}

[a]Compact tension specimens (1TCT) from heat No. 30956 were solution annealed at 1050°C for 0.5 h (EPR = 0), and sensitized at 700°C for 12 h (EPR = 20 C/cm^2) and 700°C for 0.25 h plus 500°C for 24 h (EPR = 2 C/cm^2).

[b]The load ratio and frequency of the positive sawtooth waveform were 0.95 and 8×10^{-2} Hz, respectively.

[c]Effluent dissolved-oxygen concentration based on thallium column (conductometric) measurements. Feedwater oxygen concentration at the 0.2-ppm level was approximately a factor of ~3 higher to compensate for oxygen depletion caused by corrosion of the autoclave system.

[d]Average crack growth rates over the 1049-h period with 0.2-ppm dissolved oxygen in the feedwater were 9.0×10^{-4} and 7.9×10^{-4} mm•h^{-1}, for the EPR = 2 and 20 C/cm^2 material, respectively.

TABLE IV. Crack Growth Rate Results on Type 304 Stainless Steel (Heat No. 30956) in 289°C Water with 0.2-ppm Dissolved Oxygen and 0.1-ppm Sulfate as H_2SO_4 at an R Value of 0.95

Specimen[a] No.	EPR, C/cm^2	Frequency,[b] Hz	K_{max}, $MPa \cdot m^{1/2}$	Crack Growth Rate, $m \cdot s^{-1}$
7	0	8×10^{-2}	28.0	0
			31.2	0
			34.3	2.7×10^{-10}
			40.5	5.8×10^{-10}
			45.2[c]	5.5×10^{-10}
			49.3	7.0×10^{-10}
9	2	8×10^{-2}	30.0	1.0×10^{-10}
			35.6	2.2×10^{-10}
			41.5	3.9×10^{-10}
			50.2	5.8×10^{-10}
			55.5[c]	5.0×10^{-10}
			61.1	1.4×10^{-9}
8	20	8×10^{-2}	29.4	$\sim 1.4 \times 10^{-11}$
			33.3	1.0×10^{-10}
			36.6	3.1×10^{-11}
			41.2	9.5×10^{-11}
			41.6[c]	~0
			42.1	1.6×10^{-10}

[a]Compact tension specimens (1TCT) from heat No. 30956 were solution annealed at 1050°C for 0.5 h (EPR = 0), and sensitized at 700°C for 12 h (EPR = 20 C/cm^2) and 700°C for 0.25 h plus 500°C for 24 h (EPR = 2 C/cm^2).

[b]Frequency of the positive sawtooth waveform is based primarily on the loading time of 12 s, since the load decrease occurs within ~1 s.

[c]Sulfate was not added to the feedwater during this phase of the experiment, i.e., high-purity water with 0.2-ppm dissolved oxygen.

TABLE V. Crack Propagation Rates in Type 304 Stainless Steel (Heat No. 10285) Specimens Sensitized to Two Different Levels and Tested in 289°C Water with 8-ppm O_2

f, Hz	R	K_{max}, MPa·m$^{1/2}$	Crack Growth Rate, m·s^{-1}
	EPR = 1.4 C/cm^2		
0	1.0	33-34	1.2×10^{-10}
0	1.0	36-37	2.9×10^{-10}
0	1.0	37-38	4.5×10^{-10}
1×10^{-3}	0.5	31-32	2.6×10^{-10}
2×10^{-3}	0.5	30-31	8.9×10^{-10}
	0.5	30-33	3.4×10^{-9}
	0.6	32-33	6.6×10^{-10}
	0.7	30-31	3.4×10^{-10}
	0.7	32-33	5.9×10^{-10}
	0.79	31-32	5.5×10^{-10}
	0.79	34-36	5.4×10^{-10}
	0.8	29-32	7.4×10^{-10}
	0.8	30-31	4.4×10^{-10}
1×10^{-1}	0.94	30-31	3.1×10^{-10}
1×10^{-1}	0.94	31-32	1.9×10^{-10}
2×10^{-3}	0.95	35-36	1.7×10^{-10}
	0.95	36-37	1.5×10^{-10}
	0.95	38-39	2.0×10^{-10}
	0.95	39-40	3.1×10^{-10}
	EPR = 1.8 C/cm^2		
0	1.0	32-33	2.2×10^{-10}
2×10^{-3}	0.5	30-32	2.8×10^{-9}
2×10^{-3}	0.6	28-29	5.6×10^{-10}
1×10^{-1}	0.94	30	2.1×10^{-10}

Fig. 1. Dependence of Crack Growth Rate on Stress Intensity Factor, K_{max}, for Moderately Sensitized (EPR = 20 C/cm^2) Type 304 SS in High-Purity Water with 8-ppm Dissolved Oxygen at 289°C. Steady-state crack growth rates were obtained at an R value of 0.95 with a positive sawtooth waveform, in which the frequency was determined by the slow loading time.

Fig. 2. Crack Length versus Time for 1TCT Specimens of Solution-annealed (EPR = 0) and Sensitized (EPR = 2 and 20 C/cm^2) Type 304 SS in 289°C Water Containing 0.2-ppm Dissolved Oxygen, with an Intermediate Period in Which the Oxygen Concentration Was Decreased to 0.02 ppm. The loading conditions for the positive sawtooth waveform with a slow loading time (12 s) and rapid unloading (1 s) are as follows: stress ratio R = 0.95, frequency = 8 x 10^{-2} Hz, and K_{max} = 29 to 32 MPa•m$^{1/2}$ for the specimen with the largest crack.

Fig. 3. Crack Length vs Time for 1TCT Specimens of Solution-annealed (EPR = 0) and Sensitized (EPR = 2 and 20 C/cm^2) Type 304 SS in 289°C Water Containing 0.2-ppm Dissolved Oxygen and 0.1-ppm Sulfate as H_2SO_4. The loading conditions for the positive sawtooth waveform with a slow loading time (12 s) and rapid unloading (1 s) are as follows: stress ratio R = 0.95, K_{max} = 28 MPa•m$^{1/2}$, and frequency = 8 x 10^{-2} Hz.

Fig. 4. Crack Length versus Time for 1TCT Specimens of Solution-annealed (EPR = 0) and Sensitized (EPR = 2 and 20 C/cm^2) Type 304 SS in 289°C Water Containing 0.2-ppm Dissolved Oxygen and 0.1-ppm Sulfate as H_2SO_4, Except for an Intermediate Period with High-Purity Water. The loading conditions for the positive sawtooth waveform with a slow loading time (12 s) and a rapid unloading (1 s) are as follows: stress ratio R = 0.95, frequency = 8 x 10^{-2} Hz, and K_{max} = 49 to 63 MPa•m$^{1/2}$ for the specimen with the largest crack.

Fig. 5. Effect of Stress Intensity Factor on the Crack Growth Rate of Type 304 SS in 289°C Water with 0.2-ppm Dissolved Oxygen and 0.1-ppm Sulfate as H_2SO_4. Steady-state crack growth rates were obtained at a frequency and load ratio of 8 x 10^{-2} Hz and 0.95, respectively, for a positive sawtooth waveform.

Fig. 6. Comparison of Measured Crack Growth Rates with Those Predicted by Superposition of Power Law Representations for SCC Growth and Fatigue Crack Growth [Eq. (1)].

Fig. 7. Comparison of Measured Crack Growth Rates with Those Predicted by Superposition of Power Law Representations for SCC Growth and Fatigue Crack Growth [Eq. (8)].

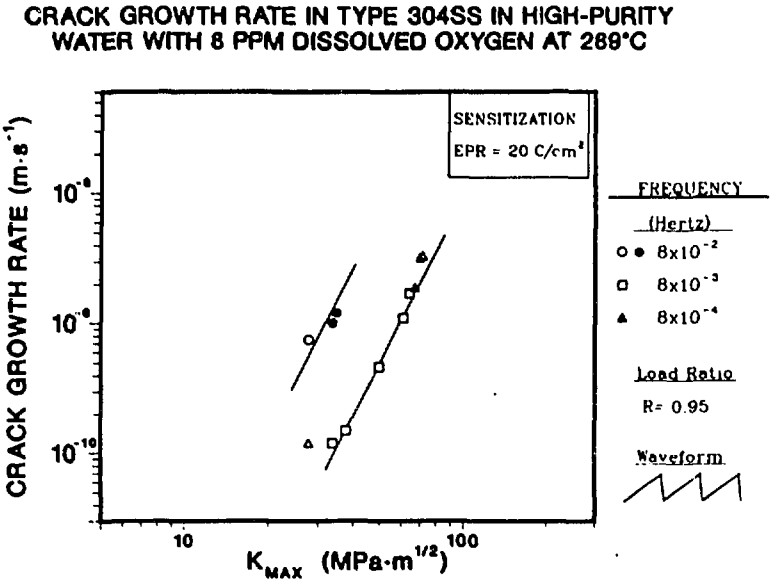

Fig. 1. Dependence of Crack Growth Rate on Stress Intensity Factor, K_{max}, for Moderately Sensitized (EPR = 20 C/cm^2) Type 304 SS in High-Purity Water with 8-ppm Dissolved Oxygen at 289°C. Steady-state crack growth rates were obtained at an R value of 0.95 with a positive sawtooth waveform, in which the frequency was determined by the slow loading time.

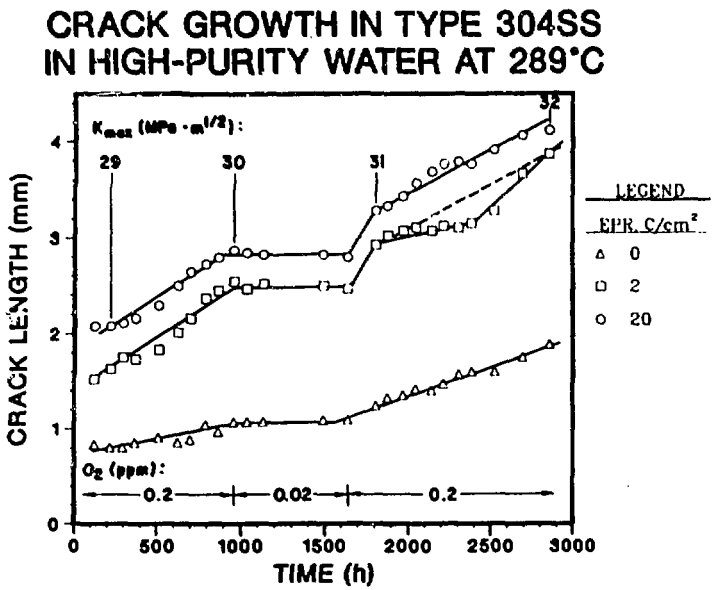

Fig. 2. Crack Length versus Time for 1TCT Specimens of Solution-annealed (EPR = 0) and Sensitized (EPR = 2 and 20 C/cm^2) Type 304 SS in 289°C Water Containing 0.2-ppm Dissolved Oxygen, with an Intermediate Period in Which the Oxygen Concentration Was Decreased to 0.02 ppm. The loading conditions for the positive sawtooth waveform with a slow loading time (12 s) and rapid unloading (1 s) are as follows: stress ratio R = 0.95, frequency = 8 x 10^{-2} Hz, and K_{max} = 29 to 32 MPa·m$^{1/2}$ for the specimen with the largest crack.

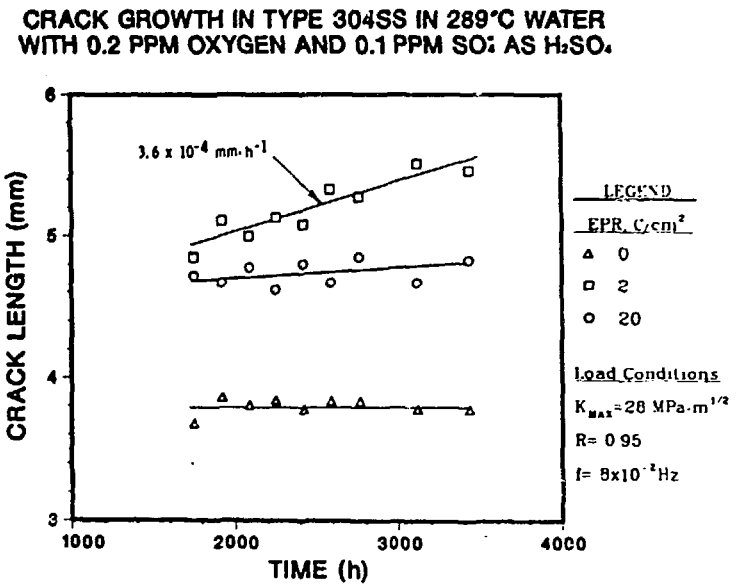

Fig. 3. Crack Length vs Time for 1TCT Specimens of Solution-annealed (EPR = 0) and Sensitized (EPR = 2 and 20 C/cm^2) Type 304 SS in 289°C Water Containing 0.2-ppm Dissolved Oxygen and 0.1-ppm Sulfate as H_2SO_4. The loading conditions for the positive sawtooth waveform with a slow loading time (12 s) and rapid unloading (1 s) are as follows; stress ratio R = 0.95, K_{max} = 28 $MPa \cdot m^{1/2}$, and frequency = 8 x 10^{-2} Hz.

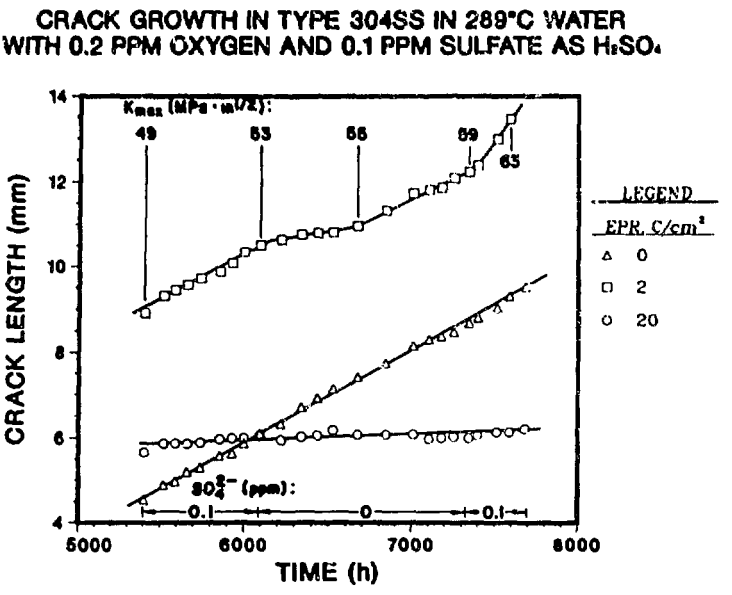

Fig. 4. Crack Length versus Time for 1TCT Specimens of Solution-annealed (EPR = 0) and Sensitized (EPR = 2 and 20 C/cm^2) Type 304 SS in 289°C Water Containing 0.2-ppm Dissolved Oxygen and 0.1-ppm Sulfate as H_2SO_4, Except for an Intermediate Period with High-Purity Water. The loading conditions for the positive sawtooth waveform with a slow loading time (12 s) and a rapid unloading (1 s) are as follows: stress ratio R = 0.95, frequency = 8×10^{-2} Hz, and K_{max} = 49 to 63 $MPa \cdot m^{1/2}$ for the specimen with the largest crack.

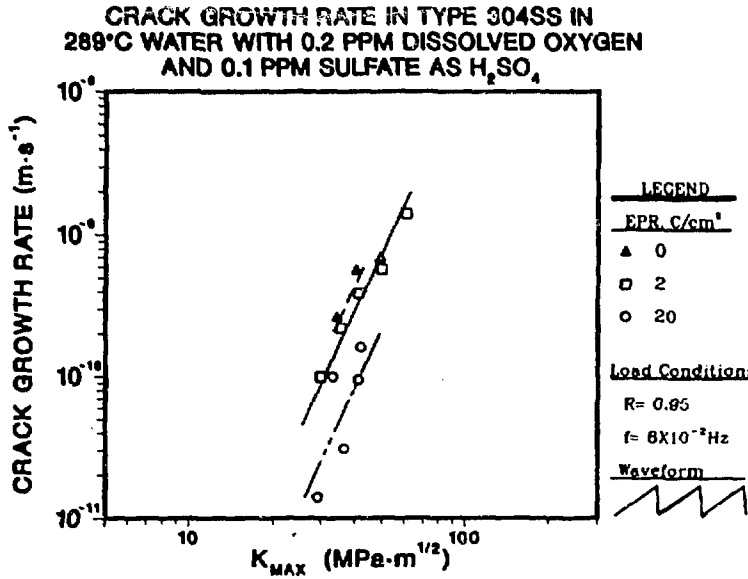

Fig. 5. Effect of Stress Intensity Factor on the Crack Growth Rate of Type 304 SS in 289°C Water with 0.2-ppm Dissolved Oxygen and 0.1-ppm Sulfate as H_2SO_4. Steady-state crack growth rates were obtained at a frequency and load ratio of 8×10^{-2} Hz and 0.95, respectively, for a positive sawtooth waveform.

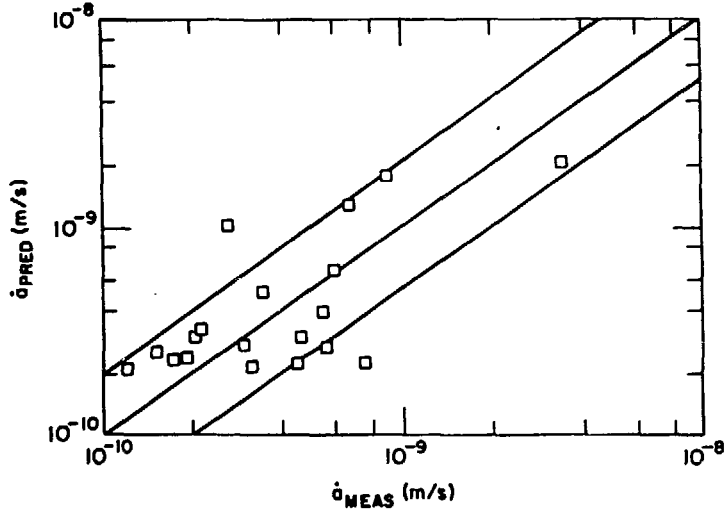

Fig. 6. Comparison of Measured Crack Growth Rates with Those Predicted by Superposition of Power Law Representations for SCC Growth and Fatigue Crack Growth [Eq. (1)].

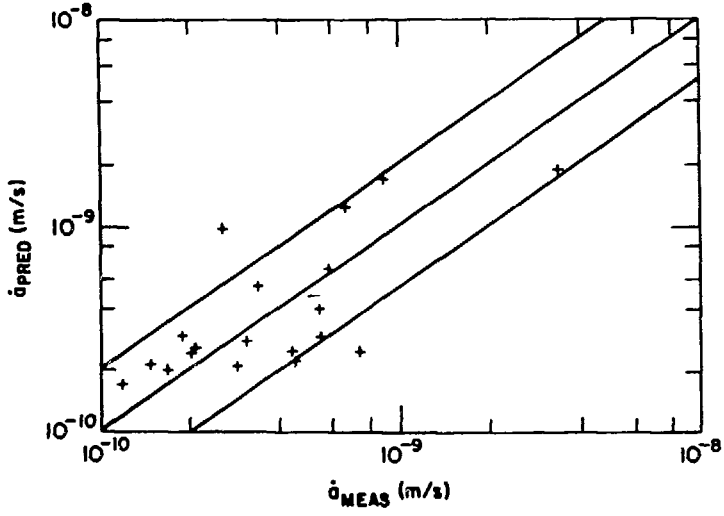

Fig. 7. Comparison of Measured Crack Growth Rates with Those Predicted by Superposition of Power Law Representations for SCC Growth and Fatigue Crack Growth [Eq. (8)].